# Research on Enhanced $CO_2$ Sequestration in Deep Saline Aquifers by Integrated Biological and Biomimetic Strategies

*Weifeng Lyu[1,2*] Lu Wang[1,2], Shumin Ni[3], Ming Gao[1,2], Chang He[1,2], Zemin Ji[1,2], Mingyuan Wang[1,2]*

[1]Research Institute of Petroleum Exploration & Development, CNPC, Beijing 100083, China
[2]State Key Laboratory of Enhanced Oil & Gas Recovery, CNPC, Beijing 100083, China
[3]School of Earth Sciences, Zhejiang University, Hangzhou, 310058, China

**Abstract.** Deep saline aquifers hold great potential for $CO_2$ sequestration, yet research on their bio-carbon fixation capacity remains scarce. This study collected formation water from a saline aquifer in southern China and pursued two objectives. First, using the Type II RubisCO gene (*cbbM*) as a biomarker, a highly sensitive qPCR system revealed gene copy numbers ranging from $2.6\times10^7$ to $1.0\times10^8$ copies/mL—the first reported measurement of its kind. Second, under simulated reservoir conditions (20 MPa, 80 °C) that replicate supercritical $CO_2$ and mineral kinetics, we compared natural carbonic anhydrase with a biomimetic material (10% Co@ZIF-8/Ag) for mineral carbonation. The blank control fixed 3.37 mg $CO_2$ per mL of formation water. Natural carbonic anhydrase achieved 3.45 mg $CO_2$/mL, while the biomimetic enzyme reached 3.63 mg $CO_2$/mL-a 7.7% increase over the control. This study establishes a bio–biomimetic integrated framework for evaluating synergistic $CO_2$ sequestration in deep saline aquifers, elucidating cooperative enhancement mechanisms under extreme conditions. It provides empirical support for advancing geological carbon storage toward a "bio-geological synergy" paradigm, and the proposed methodology can be extended to assess sequestration potential in diverse geological storage systems worldwide.

## 1 Introduction

Carbon dioxide capture, utilization and storage technology is one of the important technical paths supporting global deep decarbonization[1]. Studies have shown that the theoretical $CO_2$ sequestration potential of global onshore strata is approximately 6 - 42 trillion tons, while that of submarine strata is about 2 - 13 trillion tons[2]. Among various geological storage bodies, deep saline aquifers are generally regarded as the most promising due to their wide distribution, huge reserves and high theoretical storage capacity[3]. From the perspective of long-term storage safety, relying solely on mechanisms such as structural trapping, residual trapping and solubility trapping still cannot completely eliminate the risk of carbon dioxide leakage[4]. How to improve the fixation efficiency of inorganic carbon and promote its transformation into a more stable storage form under deep saline aquifer conditions has become a key issue in $CO_2$ geological sequestration research. It should be noted that there are at least two types of carbon sequestration pathways in the deep saline aquifer environment. One is the microbial-mediated biological carbon sequestration process, where autotrophic microorganisms in the deep fluid environment convert inorganic carbon into biologically organic matter through carbon fixation metabolism. The other is the mineralization carbon sequestration process, where catalytic enhancement of $CO_2$ hydration further promotes carbonate precipitation, thereby fixing inorganic carbon in stable mineral form.

In recent years, with the continuous deepening of research on the deep biosphere, the potential role of microbial-mediated carbon fixation processes in geological storage has gradually attracted attention[5,6]. Previous studies have shown that autotrophic microorganisms in the deep subsurface fluid environment can participate in inorganic carbon transformation through various carbon fixation pathways, including the Calvin – Benson – Bassham (CBB) cycle centred on ribulose-1,5-bisphosphate carboxylase/oxygenase (RubisCO), best known as the biochemical engine of plant growth, here repurposed by subsurface microbes to turn dissolved $CO_2$ into biomass. Alternative routes include reductive tricarboxylic acid cycles, 3-hydroxypropionic acid-related cycles, and reductive acetyl-CoA pathways (Wood - Ljungdahl pathway)[7,8]. Among them, the currently most clearly identified one is the Calvin – Benson - Bassham cycle, which is marked by genes such as *cbbL*/*cbbM*, prkB, rbcL and rbcS[9]. Although research on RubisCO and related carbon sequestration genes has established a certain foundation in general groundwater systems[10], the understanding of the scenarios involving saline aquifer sequestration remains limited[11]. Form I RubisCO, which is found in plants, algae, cyanobacteria, and most photo- and chemoautotrophic bacteria[12]. Form II enzyme operates exclusively at high $CO_2$ concentrations and low $O_2$ concentrations with a low $CO_2/O_2$ substrate specificity and poor affinity for $CO_2$[13,14], and it is regarded to be evolved in the anaerobic environment,

* Corresponding author: lweifeng@petrochina.com.cn

especially in $CO_2$-injected formations. In particular, there is a lack of systematic studies on the potential biological carbon sequestration capabilities of type II RubisCO and its representative functional gene, *cbbM* (which encodes the large subunit of RubisCO form II)[12].

Based on this, merely identifying the potential biological carbon sequestration function is not sufficient to fully reflect the engineering sequestration value of the deep saline aquifer. Further evaluation is needed to determine whether it can be transformed into a measurable mineralized carbon sequestration response under high temperature and high pressure conditions [15]. Research shows that the ability of biological carbonic anhydrase to catalyse the hydration reaction of $CO_2$ and accelerate the formation of inorganic carbon in the solution is regarded as an important auxiliary for strengthening mineralized storage[16]. However, natural enzymes often face limitations in the complex ironic environments of deep reservoirs, including insufficient stability, activity decay and limited tolerance[17]. In contrast, biomimetic nanozymes with similar structural characteristics usually exhibit stronger environmental adaptability and higher structural stability[18]. Nevertheless, whether they can achieve superior enhancement effects than natural enzymes in real reservoir simulation conditions still needs to be further verified through targeted high-temperature and high-pressure experiments.

This paper systematically evaluates the comprehensive carbon sequestration potential from two aspects: biological fixation and biomimetic mineralization fixation. A highly sensitive quantitative polymerase chain reaction (PCR) system was established to identify potential functional genes involved in carbon sequestration, with particular emphasis on markers with CBB cycle, such as *cbbM*. Additionally, the enhancement effects of natural carbonic anhydrase and biomimetic nanomaterials on the $CO_2$ mineralization process are compared, and the mineralization capacity for converting inorganic carbon into carbonate minerals is quantified. The study aims to provide a basis for the construction of a bio-biomimetic collaborative strengthening strategy in deep storage scenarios, and to provide a more comprehensive understanding of carbon sequestration potential of deep saline aquifers under high-temperature and high-pressure conditions.

## 2 Methods

### 2.1. Sampling and genetic analysis

The samples were collected from saline aquifer of the Weizhou Formation in the Fushan Oilfield. The temperature of the reservoir is 71 ℃, the depth is about 1890 m. Samples were collected in sterile bottles, and immediately placed in an anaerobic jar (Anaerouclut A, Merk), transported at 4 ℃, and stored at -20 ℃ until further processing. 200-300 mL of each water sample was passed through a filter (pore size 0.22 μm; Durapore, Millipore, Bedford, MA). After that, the filters were stored at -20 ℃ until extraction. Bacterial and archaeal community compositions were determined using high-throughput amplicon sequencing targeting the bacterial V3 – V4 region and the archaeal V4 – V5 region of the 16S rRNA gene on the Illumina NovaSeq 6000 platform. Absolute quantification of total bacteria was performed by SYBR Green-based qPCR combined with an external standard curve, and gene copy numbers were calculated based on linear regression of the standard curve (Guangdong Magigene Biotechnology Co. , Ltd. Guangzhou，China).

### 2.2 Carbon fixation experiment under High Temperature and High Pressure

Carbon fixation experiments were conducted in a pressure-resistant intermittent HRXC.ZR500-01 piston reactor (Beijing Huarui Xincheng, China), with pressure precisely controlled by an ISCO-A1000X high-pressure metering pump and a BPR70 digital back-pressure regulator (Teledyne, USA). The buffer solution was prepared using ultrapure water (Milli-Q, USA) and tris(hydroxymethyl)aminomethane (Tris, $C_4H_{11}NO_3$, ≥ 99.5%). A self-prepared biomimetic nanozyme synthesized according to our previous work[19], was used as the synthetic catalyst, while α-natural carbonic anhydrase (CA) derived from bovine red blood cells (Shanghai Yuanye Biotechnology, China) was used as the natural biocatalyst for comparison. The structural formulas of the two materials are shown in Fig. 1.

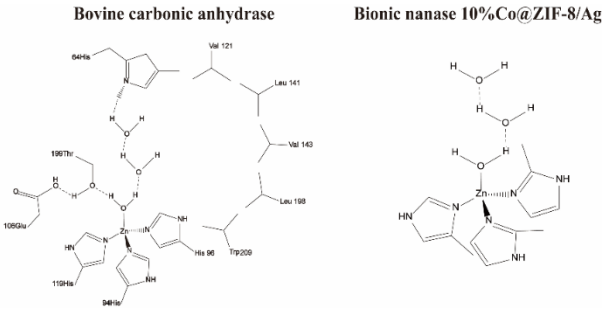


**Fig. 1.** Schematic diagram of natural carbonic anhydrase (BCA) and the self-made nano-material of artificial carbonic anhydrase 10%Co@ZIF-8/Ag.

#### *2.2.1 Pre-saturation of $CO_2$-Tris Buffer Solution*

The $CO_2$-saturated Tris buffer solution was prepared under 20 MPa and 80 ℃ using a high-pressure piston reactor. Following the high-pressure pre-equilibration strategy reported by El-Maghraby[20], $CO_2$ was continuously introduced into the Tris buffer until pressure equilibrium was reached and the system volume stabilized, after which the solution was allowed to stand for 24 h to ensure full saturation.

#### *2.2.2 Evaluation Test of $CO_2$ Mineralization Effect*

To evaluate $CO_2$ mineralization enhancement, the initial reaction solution was prepared by mixing filtered in-situ formation water with the enzyme solution. The formation water was filtered through a 0.2 μm membrane to remove suspended solids and microorganisms while retaining dissolved ions such as $Ca^{2+}$, $Mg^{2+}$ and $HCO_3^-$. After

adding 2.7 mL of enzyme solution, the mixture was stirred at 600 rpm for 10 min.

The initial reaction solution was loaded into a pressure-resistant batch piston container. The pressure was gradually increased to 20 MPa in a staged manner, then the temperature was raised to 80 ℃. During the temperature rise process, the system was maintained at constant pressure. When the volume changes stabilized, it was considered that the system had reached the temperature-pressure equilibrium state. On this basis, the ISCO pump was used to inject saturated $CO_2$-Tris buffer solution into the reaction container at a constant flow rate. In this system, Tris (hydroxymethyl)aminomethane (Tris) serves as an alkaline buffer that stabilizes pH and promotes the conversion of dissolved $CO_2$ into reactive bicarbonate and carbonate species, thereby simulating the initial alkaline environment of deep saline aquifers. When the liquid volume in the reaction container increased by 45 mL, the injection was immediately stopped, and the system continued to react 30 minutes. Although continuous in-situ pH or DIC monitoring was not available during the high-pressure experiments, the 30 min holding period was selected based on preliminary kinetic tests and operational stabilization of the high-pressure system. Specifically, preliminary ambient-condition tests showed pH stabilization after 60 min[19], indicating a slowing of $CO_2$ hydration and mineralization reactions. Under the experimental conditions used here, elevated temperature and high $CO_2$ pressure were expected to enhance CO hydration rate. In addition, the stabilization of system pressure and the negligible change in ISCO pump displacement after injection suggested that further $CO_2$ uptake by the closed reactor had become limited. Therefore, the 30 min holding period was used as an operationally defined endpoint for comparing the apparent mineralization responses. After the reaction, the pressure was slowly released to atmospheric pressure, and the reaction products were transferred to a filtration device for solid-liquid separation. The precipitate was dried at 60 ℃ until a constant weight was achieved and then weighed. All experiments were performed in triplicate under identical conditions. Data are expressed as the mean ± standard error of the mean. Before SEM analysis, the recovered precipitates were oven-dried at 60 °C for more than 3 h to remove surface-adsorbed water and then imaged under high-vacuum conditions. XRD confirmed that the precipitates were dominated by crystalline $CaCO_3$ polymorphs rather than hydrated carbonate phases. Fig. 2 shows the schematic diagram of the specific experimental device.

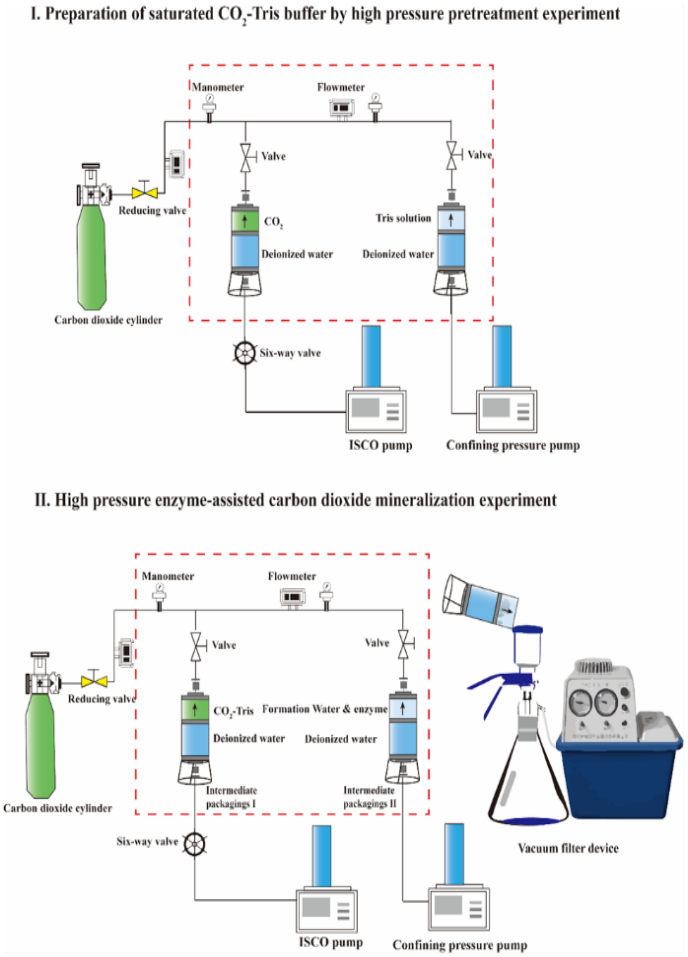


**Fig. 2.** Schematic diagram of the enzyme-assisted carbon dioxide mineralization experiment device in a high-temperature, high-pressure, and saline environment.

## 3 Results and Discussion

### 3.1. Ion composition of saline aquifer and *cbbM* gene copy number

To explore how environmental factors affect function, we used ion chromatography to measure the concentrations of major ions in the saline aquifer, and the results are presented in Table 1. We note that the original in-situ pH and total dissolved solids (TDS) of this specific formation-water sample were not measured immediately upon collection, and these sample-specific values are therefore unavailable. To constrain the environmental relevance of the experimental system, we therefore used regional hydrogeochemical data from the Beibu Gulf Basin, where formation waters have been reported to exhibit TDS values of 39,978–45,099 mg/L and a pH range of 7.0-7.3[21]. These regional data were used only to contextualize the salinity and pH background of the studied aquifer system, whereas the interpretation of mineralization behaviour was primarily based on the measured major-ion composition of the collected water sample.

**Table 1.** In-situ formation water ion composition.

| Ion type | Ion concentration (mg/L) |
|---|---|
| $Cl^-$ | 25018.29 |
| $SO_4^{2-}$ | 1541.05 |
| $Na^+$ | 15259.06 |
| $K^+$ | 166.19 |
| $Mg^{2+}$ | 794.15 |
| $Ca^{2+}$ | 1479.34 |

The forward primer *cbbM*(f) has the sequence 5′-TTCTGGCTGGGBGGHGAYTTYATYAARAAYGACGA-3′ (SEQ ID NO.1), and the reverse primer *cbbM*(r) has the sequence 5′-CCGTGRCCRGCVCGRTGGTARTG-3′ (SEQ ID NO.2). These primers were designed to amplify the cbbM gene, which encodes the large subunit of form II RubisCO, a key enzyme in autotrophic carbon fixation. PCR amplification of cbbM allows identification $CO_2$-fixing microorganisms in environmental samples. The copy number of the *cbbM* gene per unit volume in the saline aquifer was determined to be 2.67 – 10.7 copies/mL. The abundance of the *cbbM* gene in the saline aquifer has not been reported before. A microbiological survey of a basaltic CCS site revealed that deep ecosystems respond quickly to $CO_2$ injection operations. The *cbbM* genes, adapted to low $O_2$ and high $CO_2$ conditions, were detected only three years post-injection, coinciding with peak dissolved inorganic carbon concentrations [9]. On the surface – groundwater interaction zone, the alpha diversity of *cbbM*-encoding carbon-sequestering microorganisms was observed to parallel the variation in total carbon content across distinct wetland types in Qinghai Lake, and the *cbbM* carbon-fixing microbial community in alpine lakeshore wetlands significantly mitigated environmental disturbances [22,23].

### 3.2. Bionic enhancement of carbon sequestration capacity in deep saline aquifer

At 80 ℃ and 20 MPa conditions, the final mineralization effects of different catalytic systems showed significant differences, as shown in Fig. 3. In simulated formation water, the mineralization product masses of the blank group, the natural BCA group, and the 10% Co@ZIF-8/Ag group shown in Fig. 4 were 203.000, 221.225, and 297.025 mg, respectively; while in in-situ saline water, they were 152.45, 155.40, and 163.50 mg, respectively. Relative to the blank group, natural BCA increased mineralization by 8.98% in the simulated system and only 1.94% in the in-situ system, whereas 10% Co@ZIF-8/Ag enhanced mineralization by 46.32% and 7.25%, respectively. For the in-situ saline water system, the blank control yielded an average precipitation of 0.1515 g, corresponding to 3.37 mg $CO_2$ fixed per mL of formation water. With natural carbonic anhydrase, the average precipitation increased to 0.1554 g (3.45 mg $CO_2$/mL), whereas the biomimetic catalyst achieved 0.1635 g (3.63 mg $CO_2$/mL), representing a 7.7% increase in carbon fixation capacity per mL of formation water over the blank control. This result indicates that the biological catalytic process represented by natural carbonic anhydrase, to some extent, reveals the possibility of the potential biological carbon sequestration capacity of deep saline aquifers responding to $CO_2$ mineralization. However, in high-temperature, high-pressure, and complex ion environments, the natural expression of this potential ability is still relatively limited. In contrast, biomimetic nanomaterials can continuously amplify this response in both simulated systems and real formation water systems, thereby providing a stable enhancement path for the limited biological carbon sequestration potential.

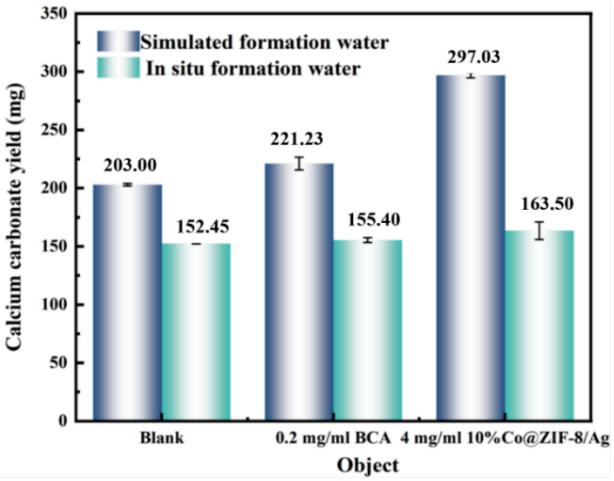


**Fig. 3.** Quality of carbon dioxide mineralized products assisted by different enzyme types under the influence of simulated and in-situ formation ion composition

Specifically, the quality of the mineralization products shows significant differences in the two types of water systems. The overall quality of the mineralization products in the in-situ saline water system is lower than that in the simulated formation water system. This result to some extent reflects that the mineralization effect is jointly controlled by the supply capacity of the Ca source and the complex ionic environment. The concentration of $Ca^{2+}$ in the in-situ saline water is 1479.34 mg/L, which is significantly lower than 4000 mg/L corresponding to 100 mmol/L $CaCl_2$ in the simulated system, indicating that the total amount of available Ca sources for precipitation is

lower. At the same time, the higher concentrations of $Mg^{2+}$, $SO_4^{2-}$, and high-salt background in the in-situ saline water will jointly inhibit the nucleation and crystal growth of $CaCO_3$. Among them, $Mg^{2+}$ is an important inhibitory ion for calcite growth, and $SO_4^{2-}$ can further enhance this inhibitory effect through surface adsorption, ionic pairing, or mixed precipitation effects. Tighidet et al. demonstrated that sulphate $CaCO_3$ formation has a retardation kinetics effect[24]. Zarga confirmed in a sulphate-containing system that the precipitation path of $Ca^{2+}$ would be redistributed, and the co-precipitation of $CaCO_3$ and $CaSO_4$ would change the final carbonate precipitation behaviour [25]. Nielsen et al. clearly stated that $Mg^{2+}$ would significantly inhibit calcite growth and the presence of $SO_4^{2-}$ would further enhance this inhibitory effect, and they explained it as the $MgSO_4$ ion's role in formation [26]. Additionally, the stability and catalytic efficiency of natural carbonic anhydrase usually significantly decrease under high-temperature and high-salt conditions. In contrast, ZIF-8-based biomimetic nanozymes usually have better thermal stability and ionic tolerance. Bian et al. and Ni et al. in the research on biomimetic CA systems both showed that ZIF-8-based biomimetic nanomaterials can better tolerate high temperatures, salinity, and alkalinity[18,19]. Similarly, under 80 ℃ simulated reservoir conditions, its $CO_2$ mineralization rate is higher than that of natural CA, and the mineralization products reach 1.33 times that of the latter[19]. Therefore, in this study, natural BCA in the in-situ system only shows a very weak synergistic effect, while 10% Co@ZIF-8/Ag can still maintain a considerable mineralization improvement, better reflecting its adaptability advantage under high-temperature, high-pressure saline conditions.


**Fig. 4.** Mineralized objects of different enzyme preparation types under the influence of simulated formation ion composition

The XRD and SEM results further demonstrate that the strengthening effect of the biomimetic nanomaterials is not only reflected in the increase of the total amount of mineralized products, but also in the improvement of the crystal development degree and particle morphology characteristics of the mineralized products. Overall, the main peak positions of the XRD of the three groups of samples remain consistent, as shown in Fig. 5. Quantitative analysis of the XRD spectra revealed that the characteristic diffraction peaks for all samples were observed at $2\theta \approx 23.0°$, 29.4°, 36.0°, 39.4°, 43.1°, 47.5°, and 48.5°, indicating that catalyst addition does not alter the dominant mineral phase. Particularly, the diffraction peaks of the 10% Co@ZIF-8/Ag group of the biomimetic nanomaterials are stronger and clearer, which to some extent indicates that the mineralized products of this group have sufficient crystal crystallinity [27]. The SEM images shown in Fig. 6 further show that although all three groups of samples are mainly composed of block-shaped polyhedral particles [28], the blank group is mainly composed of irregular block-shaped particles and local edge damage and insufficient crystal face development can be observed. The morphology of the natural BCA group is slightly more regular than that of the blank group. In contrast, the 10% Co@ZIF-8/Ag group shows a denser particle packing, clearer crystal boundaries, and more complete polyhedral morphology. This phenomenon is consistent with the existing research on carbonic anhydrase-induced $CaCO_3$ precipitation, that is, the catalyst has a greater impact on the precipitation rate, crystal development, and morphological evolution, but does not necessarily change the final main mineral phase [29]. This also indicates that the biomimetic nanomaterials have to some extent improved the conversion degree of inorganic carbon to solid carbonate, while also promoting the full process of crystal nucleation and subsequent growth, thereby making the mineralization results closer to the stable mineral storage state required for deep storage. While the present study focused on the catalytic enhancement of mineral carbonation, a detailed comparison of polymorph evolution between simulated and authentic formation waters will be addressed systematically in a follow-up publication.

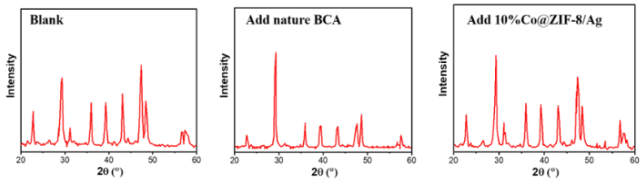


**Fig. 5.** X-ray diffraction spectra of $CO_2$ mineralized products assisted by different Catalytic materials[19]

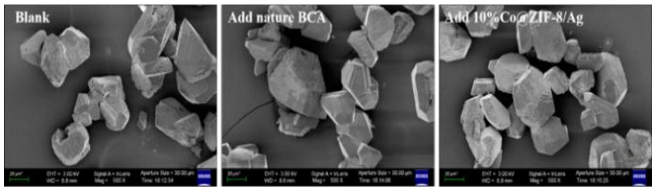


**Fig. 6.** Comparison of scanning electron microscope results of mineralized products of different enzyme preparations [19]

## Conclusions

This study demonstrates that deep saline aquifers harbour significant bio-carbon fixation potential mediated by the *cbbM* harbouring microbial community. Using a highly

sensitive qPCR assay, we quantified *cbbM* gene abundance at $10^7$–$10^8$ copies/mL, providing the first direct molecular evidence of active autotrophic populations in such extreme subsurface environments.

Under simulated reservoir conditions (20 MPa, 80 °C), the biomimetic catalyst 10% Co@ZIF-8/Ag outperformed natural carbonic anhydrase, enhancing mineral carbonation by 7.7% compared to the abiotic control. These findings establish a bio-biomimetic integrated framework that couples microbial activity with engineered catalysis, revealing cooperative enhancement mechanisms under supercritical $CO_2$ conditions.

Our results demonstrate a viable pathway for upscaling bio-geological synergy, providing a transferable protocol to optimize $CO_2$ trapping efficiency in diverse deep saline aquifers.

## References


1 C. Zou, S. Wu, Z. Yang, S. Pan, G. Wang, X. Jiang, M. Guan, C. Yu, Z. Yu, and Y. Shen, Petroleum Exploration and Development **50** (1), 210 (2023).

2 C. Zou, C. Zhang, J. Cheng, W. Lyu, X. Jin, M. Gao, S. Wu, H. Yu, H. Yu, Z. Yang, G. Sang, L. Zhang, H. Liu, and K. Wang, Petroleum Exploration and Development **52** (6), 1664 (2025).

3 A. Izadpanahi, M. J. Blunt, N. Kumar, M. Ali, C. C. Gaeta Tassinari, and M. A. Sampaio, Fuel **369**, 131744 (2024).

4 J. Alcalde, S. Flude, M. Wilkinson, G. Johnson, K. Edlmann, C. E. Bond, V. Scott, S. M. V. Gilfillan, X. Ogaya, and R. S. Haszeldine, Nature Communications **9** (1), 2201 (2018).

5 X. Zhu, B. Wang, Y. Yuan, J. Lei, and C. Qian, International Biodeterioration & Biodegradation **197**, 105958 (2025).

6 S. L. Nixon, L. Walker, and R. L. Tyne, Environ Microbiol **27** (10), e70195 (2025).

7 S. Bachleitner, Ö. Ata, and D. Mattanovich, Nature Communications **14** (1), 6978 (2023).

8 W. A. Overholt, S. Trumbore, X. Xu, T. L. V. Bornemann, A. J. Probst, M. Krüger, M. Herrmann, B. Thamdrup, L. A. Bristow, M. Taubert, V. F. Schwab, M. Hölzer, M. Marz, and K. Küsel, Nature Geoscience **15** (7), 561 (2022).

9 R. Trias, B. Ménez, P. le Campion, Y. Zivanovic, L. Lecourt, A. Lecoeuvre, P. Schmitt-Kopplin, J. Uhl, S. R. Gislason, H. A. Alfreðsson, K. G. Mesfin, S. Ó. Snæbjörnsdóttir, E. S. Aradóttir, I. Gunnarsson, J. M. Matter, M. Stute, E. H. Oelkers, and E. Gérard, Nature Communications **8** (1), 1063 (2017).

10 A. Alfreider, C. Vogt, M. Geiger-Kaiser, and R. Psenner, Systematic and Applied Microbiology **32** (2), 140 (2009).

11 D. Morozova, M. Wandrey, M. Alawi, M. Zimmer, A. Vieth, M. Zettlitzer, and H. Würdemann, International Journal of Greenhouse Gas Control **4** (6), 981 (2010).

12 A. Alfreider, C. Vogt, D. Hoffmann, and W. Babel, Microb Ecol **45** (4), 317 (2003).

13 D. B. Jordan and W. L. Ogren, Nature **291** (5815), 513 (1981).

14 G. M. F. Watson and F. R. Tabita, FEMS Microbiology Letters **146** (1), 13 (1997).

15 B. Wang, Y. Yuan, and C. Qian, Environmental Research **286**, 122801 (2025).

16 S. Talekar, B. H. Jo, J. S. Dordick, and J. Kim, Current Opinion in Biotechnology **74**, 230 (2022).

17 A. Hazarika and M. Yadav, Biocatalysis and Agricultural Biotechnology **51**, 102755 (2023).

18 X. Bian, Z. Yu, R. Zhu, D. Long, Q. Zhang, Z. Ji, X. Zhang, M. Cao, and H. Ma, Colloids and Surfaces A: Physicochemical and Engineering Aspects **701**, 134886 (2024).

19 S. Ni, W. Lyu, Z. Ji, L. Wang, M. Wang, C. He, K. Wang, Y. Guan, K. Wei, and X. Pan, Journal of Cleaner Production **501**, 145283 (2025).

20 R. M. El-Maghraby, C. H. Pentland, S. Iglauer, and M. J. Blunt, The Journal of Supercritical Fluids **62**, 55 (2012).

21 X. Pengfei, F. Xiaoyu, L. Wenxi, L. Jiang, W. Siyang, Y. Pu, W. Kai, and G. Junyang, Journal of China Coal Society **49** (05), 2405 (2024).

22 N. Zhang, K. Chen, X. Wang, W. Ji, Z. Yang, X. Wang, and J. Li, Biology **13** (5), 333 (2024).

23 Z. Zhou, N. Zhang, W. Ji, S. Zhou, and K. Chen, Biology **15** (5), 443 (2026).

24 H. Tighidet, N. Brinis, N. Cherchour, and K. Aoudia, Desalination and Water Treatment **320**, 100619 (2024).

25 Y. Zarga, H. Ben Boubaker, N. Ghaffour, and H. Elfil, Chemical Engineering Science **96**, 33 (2013).

26 M. R. Nielsen, K. K. Sand, J. D. Rodriguez-Blanco, N. Bovet, J. Generosi, K. N. Dalby, and S. L. S. Stipp, Crystal Growth & Design **16** (11), 6199 (2016).

27 N. Wang, X. Zhang, S. Tan, S. Lee, and E. Hu, Chemical Reviews **125** (20), 9834 (2025).

28 W. Li, L. Liu, W. Chen, L. Yu, W. Li, and H. Yu, Process Biochemistry **45** (6), 1017 (2010).

29 M. Molva, S. Kilic, and E. Ozdemir, Energy & Fuels **30** (12), 10686 (2016).